Journal of Hydrology 603 (2021) 127141

Contents lists available at ScienceDirect

Journal of Hydrology

journal homepage: www.elsevier.com/locate/jhydrol

Impact of climate change on thermal and mixing regimes in a deep dimictic reservoir on the Qinghai-Tibetan Plateau, China

Yanjing Yang [a], Min Chen [a,*], Yun Deng [a], S. Geoffrey Schladow [b], Jia Li [a], You-Cai Tuo [a]

[a] State Key Laboratory of Hydraulics and Mountain River Engineering, Sichuan University, Chengdu 610065, China
[b] Tahoe Environmental Research Center, Department of Civil and Environmental Engineering, University of California, Davis, CA 95616, USA

ARTICLE INFO

This manuscript was handled by Marco Borga, Editor-in-Chief, with the assistance of Marco Toffolon, Associate Editor.

Keywords:
Thermal stratification
Vertical mixing
Climate change
Hypolimnetic water
Dissolved oxygen
Two-dimensional hydrodynamic model

ABSTRACT

Climate change is one of the most serious threats to aquatic ecosystems in lakes and reservoirs. Aquatic organisms on the Qinghai-Tibetan Plateau in China are particularly susceptible to changes in water temperature and hydraulic status. To better characterize the evolution of the thermal and mixing regimes of deep reservoirs under climate change on the Qinghai-Tibetan Plateau, a two-dimensional hydrodynamic model (CE-QUAL-W2) of Pangduo Reservoir was established, calibrated, and verified using observational data. We used representative concentration pathways (RCP) 2.6, 4.5, 6.0, and 8.5 based on the GFDL-ESM2M output data after bias correction using the ISIMIP2b dataset to simulate the water temperature distribution from 2021 to 2099. Our results show that Pangduo Reservoir's annual mean surface water temperature has small differences under RCP 2.6 and RCP 4.5, but there are significantly increases of 0.12 °C and 0.22 °C decade^{-1} under RCP 6.0 and RCP 8.5, respectively. The water age in the hypolimnion also increases by 0.05, 0.92, 1.73, and 3.2 d decade^{-1} under RCP 2.6, RCP 4.5, RCP 6.0, and RCP 8.5, respectively. The delay in offset of summer stratification became a key feature in response to climate warming (the longest delay change was 3.21 d decade^{-1} under RCP 8.5). Furthermore, simulated climate warming caused the compression of the spring convective periods and the strengthening of stratification in summer, which commonly weakened or even eliminated the replenishment of dissolved oxygen (DO) to the hypolimnion via vertical mixing. The depth of inflow intrusion also increased significantly (0.71 m decade^{-1} under RCP 8.5), enhancing summer thermal stratification. The increase in the depth of inflow intrusion and the extension of the age of hypolimnetic water pose potential threats to water quality and ecological health in the reservoir. The concentration of DO in the hypolimnion also significantly decreased under RCP 4.5, RCP 6.0, and RCP 8.5. These issues may also exist in other dimictic reservoirs and lakes on the Qinghai-Tibet Plateau.

1. Introduction

Climate change is one of the most serious challenges facing aquatic ecosystems worldwide (Woolway and Merchant, 2019). Lakes and reservoirs are particularly sensitive to climate and respond quickly to changes, making them important sentinels of climate change (Woolway et al., 2020). The hydrological processes, thermodynamic structure, nutritional status, and ecosystem functioning of lakes and reservoirs are all expected to respond significantly to climate warming (Caldwell et al., 2020; North et al., 2014). Thermal stratification is a key physical characteristic of lakes and reservoirs, and this is an important underlying factor driving vertical mixing of nutrients (Wang et al., 2020) and dissolved oxygen (DO) (Rogora et al., 2018) within these waterbodies. Crucially, climatic warming will affect the thermal and mixing regimes of lakes and reservoirs. It is generally believed, for example, that warming will lengthen the stratification period and make stratification more stable (He et al., 2019; Sahoo et al., 2016). The enhancement of thermal stratification will have a negative impact on aquatic organisms, thereby affecting the uses and health of affected waterbodies (Ptak et al., 2020; Weber et al., 2017). Research on the response of thermal stratification to climate change alongside other environmental effects can provide valuable insights for current and future management decisions as well as guide scientific monitoring for evaluating the impacts of climate change.

The vertical structure of many lakes and reservoirs involves a stratification-mixing mechanism across the year (Magee and Wu, 2017; Zhu et al., 2020). Periodic vertical overturning is one of the important mechanisms for replenishing DO and other substances in the deep-water

* Corresponding author.
E-mail address: mchen@scu.edu.cn (M. Chen).

https://doi.org/10.1016/j.jhydrol.2021.127141
Received 19 May 2021; Received in revised form 11 October 2021; Accepted 26 October 2021
Available online 3 November 2021

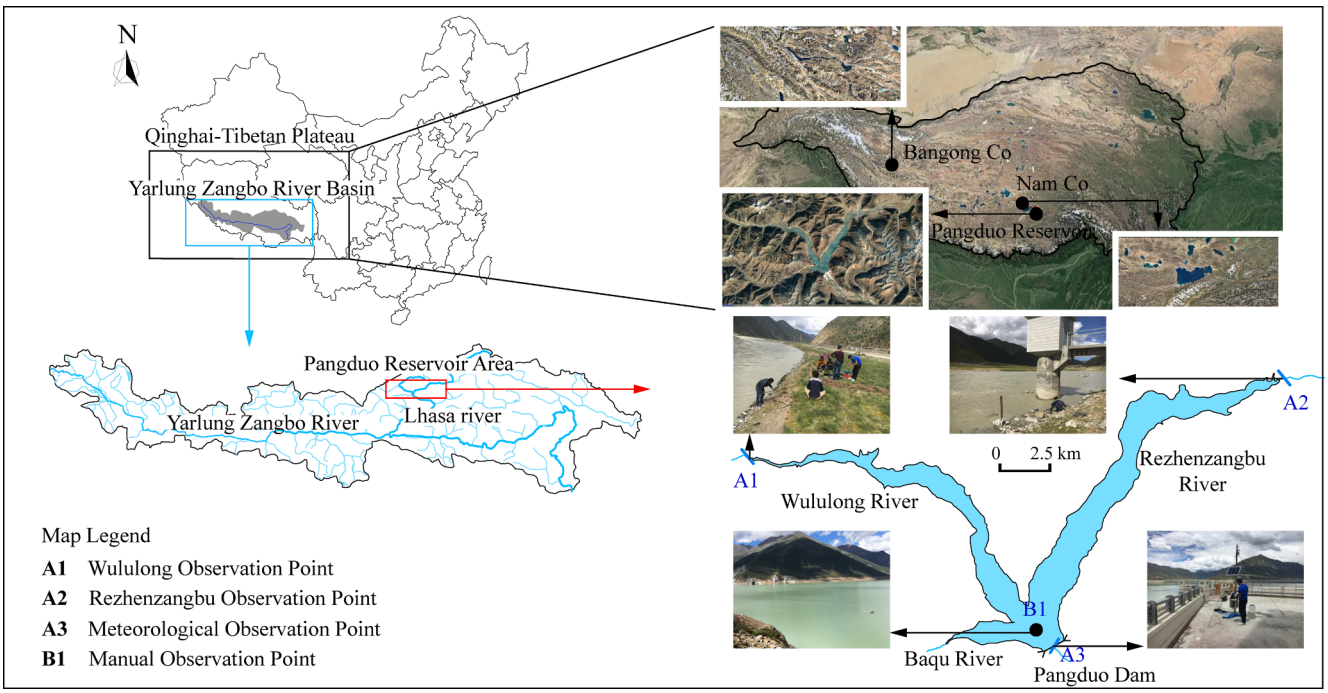

Fig. 1. Study area and locations of observation points.

layer (Schwefel et al., 2016). Therefore, the impact of climate change on such processes has large consequences for the long-term safety of the aquatic water environment (Walsh et al., 2020). As thermal expansivity increases with temperature, a stronger temperature gradient as well as a higher mean temperature increase stratification (Schwefel et al., 2016). Under current climate warming trends, slow, long-term slow warming and short-term extreme high temperatures could alter the heat-exchange rate at the air–water interface and, consequently, increase the annual heat flux in lakes (Piccolroaz et al., 2020). Although the water column warms across the entire depth range, the extent of warming diminishes with depth and strengthens stratification relative to mixing processes (Lewis et al., 2019). Such shifts in water-mixing modes make thermal stratification occur earlier in the year and prolongs the stratification period (Mi et al., 2020; Sahoo et al., 2016). This strengthened thermal stratification can lead to the occurrence of hypolimnetic hypoxia or anoxia (Sahoo et al., 2013). Furthermore, strengthened oxygen stratification promotes algal reproduction and delays fish spawning, thus affecting the structure and function of lake and reservoir ecosystems (Piccolroaz et al., 2018). Such changes also pose risks for drinking water safety and human health (Czernecki and Ptak, 2018).

The Qinghai-Tibetan Plateau (QTP) has an average altitude of 4,000 m above sea level (a.s.l.) and widely distributed lakes with a total area of over 4×10^4 km^2. Given the development of China's water conservancy projects in the source region of the QTP, the region's lakes and reservoirs are of heightened concern (Qiu, 2008). The QTP has a unique atmospheric circulation, which has an important impact on the Asian monsoon and global climate change (Ding et al., 2007). Furthermore, the aquatic ecosystem structure on the QTP is vulnerable to disruption by human impacts and environmental change (Zhu et al., 2019). For example, the aquatic organisms on the QTP grow slowly and are sensitive to changes in hydraulic conditions including water temperature and flow rate (Mengzhen et al., 2012). Therefore, the impacts of water temperature changes on the ecological environment are expected to be more significant here than in other locations. Due to its high altitude, temperature monitoring data from Bangong Co (Co means "lake" in the Tibetan language) and Nam Co (Fig. 1) on the QTP show that the lakes are dimictic (seasonally ice covered), with wind and solar radiation being the main drivers of vertical turnover (Wang et al., 2019). Simulations of Nam Co's water temperature show that under climate warming, the summer stratification-forming time advanced by approximately 4 d decade^{-1} and the summer stratification period increased by 6 d decade^{-1} (Huang et al., 2017), although stratification conditions under ice have not yet been examined.

Reservoirs are usually designed to meet specific human requirements such as flood prevention, power generation, shipping, and irrigation (Chen et al., 2016). To maximize storage potential, reservoirs commonly have large water catchment areas leading to relatively high flow rates and the presence of more concentrated particulates, nutrients, and pollutants (Hayes et al., 2017). The inflows to most reservoirs are from a main river and form a interflow intrusion with a prevailing dominant direction, whereas natural lakes tend to show a different pattern, with inflows becoming quickly mixed (Chen and Fang, 2015). While reservoirs formed by damming preexisting rivers can resemble either a storage or run-of-river system, coupled with their artificial control properties, internal mixing processes vary from natural lakes (Zarfl et al., 2015). Most studies treat reservoirs and lakes as similar waterbodies and consider their response to climate change (from a thermodynamic perspective) to be comparable. At present, however, there is little known of the thermal behavior and mixing mechanisms of dimictic reservoirs in response to climate change in high-altitude areas. Moreover, hypoxic conditions are predominantly controlled by deep mixing in winter. The decrease in the maximum mixing depth caused by climate warming directly leads to a significant decrease in DO concentrations in the hypolimnion (Li et al., 2020; Schwefel et al., 2016). Nevertheless, few studies have examined the mixing process and its influencing factors in dimictic reservoirs during the low-temperature period.

To address these gaps, this study was conducted to better understand the evolution of the thermal and mixing regimes in reservoirs in high-altitude areas under future climate change scenarios and identify the dominant factors driving these processes. We focus on Pangduo Reservoir, a run-of-river reservoir located on the QTP. We investigate changes in thermal and mixing regimes in the reservoir using the two-dimensional CE-QUAL-W2 model based on representative concentration paths (RCP) 2.6, 4.5, 6.0, and 8.5 from an ensemble of four different global climate models. We develop a characteristic index to quantify the transformation of thermal stratification and mixing mechanisms under

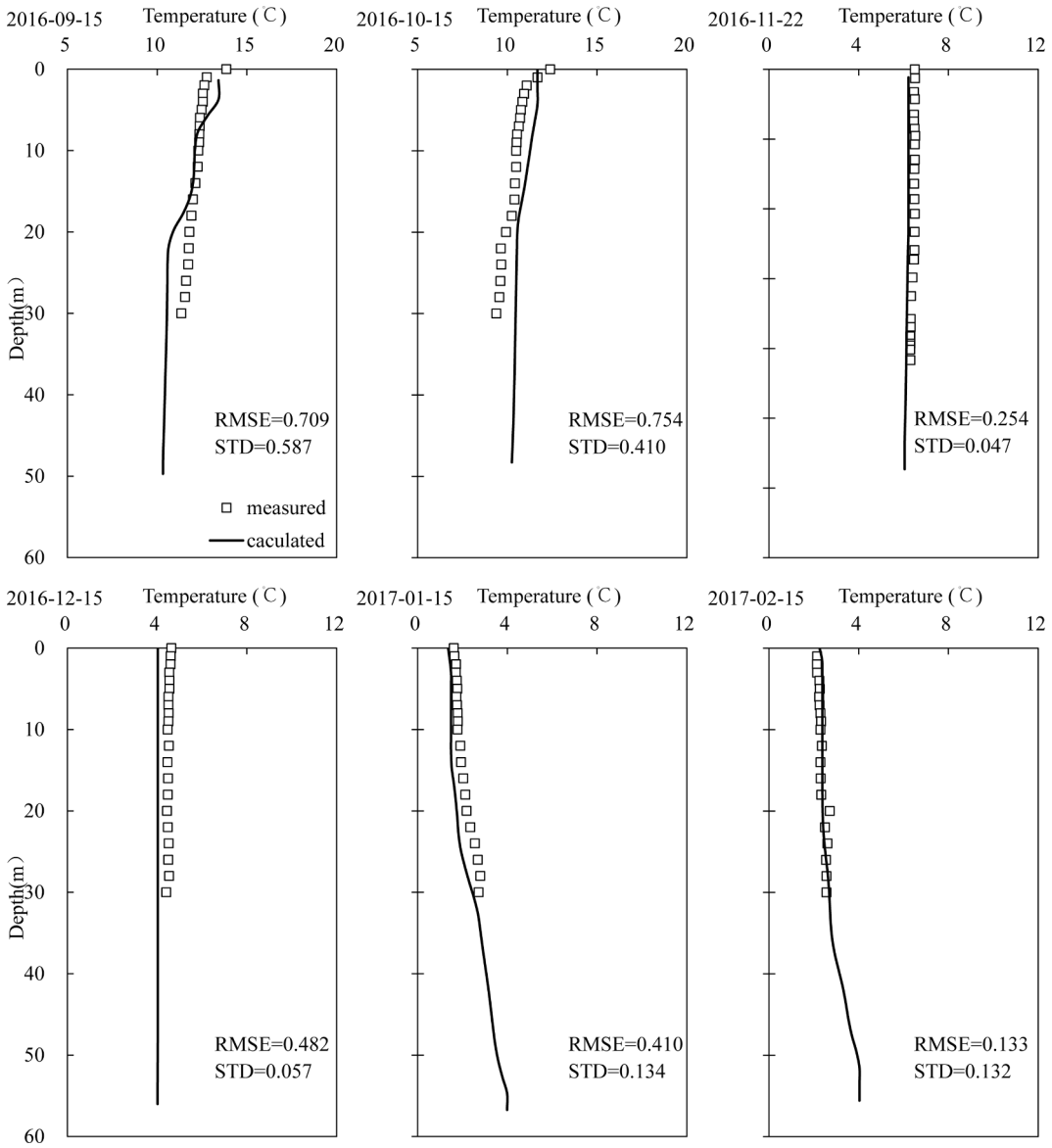

Fig. 2. Comparison of simulated and measured vertical temperature profiles upstream of Pangduo Dam.

the future climate trends, providing a scientific and theoretical reference for the adaptive management of reservoirs in the QTP region and other high-altitude areas in response to climate change.

2. Methods

2.1. Study site

Pangduo Reservoir is the largest water conservancy project in the QTP region above 4,000 m a.s.l. (Fig. 1). The height of the dam is 62 m and the elevation of the riverbed near the dam is 4,038 m a.s.l. There are two power tunnels (7-m high and 6-m wide) at Pangduo dam with an entrance bottom elevation of 4,059 m a.s.l. The full capacity of the reservoir below 4,095 m a.s.l. is 12.3×10^8 m^3.The primary functions of Pangduo Reservoir are to supply irrigation water and generate power, but the reservoir is also important for flood control, urban water supply, and ecological environmental protection. To characterize the thermal conditions in the reservoir and provide boundary conditions for model verification, we conducted water temperature and meteorological monitoring as summarized in Table S-A1.

2.2. Numerical models

We used the CE-QUAL-W2 model for our research (Cole and Buchak, 2003), a two-dimensional hydrodynamic and water quality model. While this model does not consider variations in river width, it can be applied to waterbodies with longitudinal and vertical temperature gradients such as Pangduo Reservoir. The main boundary conditions in the model are inflow, outflow, inflow water temperature, and meteorological conditions. Water density is driven by temperature, and chemical stratification is not considered here. An ice component is included in CE-QUAL-W2, which is based on an ice cover with ice-to-air heat exchange, conduction through the ice, conduction between the underlying water, and a 'melt temperature' layer at the bottom of the ice layer. This model has been widely applied to reservoirs and river impoundments worldwide. The source code is freely available (http://www.ce.pdx.edu/w2/), allowing its extension and application using new formulations and algorithms (Table S-A2). There is no input for long-wave radiation in CE-QUAL-W2, therefore we added an algorithm to read in the long-wave radiation based on modified source code.

2.2.1. Model grid and input data

The model grid is shown in Fig. S-A1, with a longitudinal size of 100–300 m and vertical size of 2 m. Meteorological input data were based on collective representative path (RCP) 2.6, 4.5, 6.0, and 8.5 of the GFDL-ESM2M model. ISIMIP2b climate data were bias-corrected for the required meteorological variables with a daily resolution based on the GFDL-ESM2M model output dataset for the period 2021–2099 (Lange, 2017; Zhao et al., 2016).

ISIMIP aimed to use the same set of climate and socioeconomic inputs to force a wide range of climate impact models using publicly available data. Currently in the second phase, ISIMIP2b, was developed in response to the Intergovernmental Panel on Climate Change (IPCC) Special Report on the 1.5 °C target, which provides the best scientific basis for political discussions about climate change mitigation and adaptation measures. ISIMIP2b data were made available publicly according to terms of use (https://www.isimip.org/protocol/terms-of-use). Bias-adjusted ISIMIP climate input data were calculated using four climate models (i.e., IPSL-CM5A-LR, GFDL-ESM2M, HadGEM2-ES, and MIROC5) at daily temporal and 0.5° horizontal resolutions (Frieler et al., 2017). These data were obtained from the Earth System Grid Federation website (https://esgf.llnl.gov/). Our climate model selection was constrained by data accuracy, which we evaluated based on historical forecasts of air temperature and measured air temperature between 1981 and 2005. The results of this assessment showed that root-mean-square errors (RMSEs) of 3.42 °C (GFDL-ESM2M), 4.39 °C (IPSL-CM5A-LR), 3.92 °C (HadGEM2-ES), and 4.13 °C (MIROC5), respectively, with corresponding coefficients of determination (R^2) of 0.8007 (GFDL-ESM2M), 0.6571 (IPSL-CM5A-LR), 0.6661 (HadGEM2-ES), and 0.6766 (MIROC5) respectively (Fig. S-A2). Based on these results, we used the GFDL-ESM2M model as a representative climate model for our predictions.

The following meteorological factors were included in the model: near-surface air temperature (tasAdjust), near-surface relative humidity (hursAdjust), near-surface wind speed (sfcWind), surface downwelling short-wave radiation (rsdsAdjust), and surface downwelling long-wave radiation (rldsAdjust) (Fig. S-A3 and Table S-A3). The annual mean air temperature increased significantly by −0.02, 0.18, 0.28, and 0.52 °C decade^{-1} under RCP 2.6, 4.5, 6.0, and 8.5, respectively. Longwave radiation was related to air temperature and showed a similar trend, with the greatest increases under RCP 8.5 (2.36 W m^{-2} decade^{-1}) and smallest increases under RCP 2.6 (0.17 W m^{-2} decade^{-1}) (Table S-A3). The reservoir operation parameters followed the designed operating conditions of the Pangduo Hydropower Station (Fig. S-A4), and the inflow, withdrawal rate, and water-level changes were assumed to be consistent over the 2021–2099 simulation period.

No inflow water temperatures were available for the ISIMIP database, but a linear regression of measured water temperatures (T_W) and observed air temperatures (T_A) (2016–2017) revealed a high correlation of $R^2 = 0.96$ ($T_W = 0.7684 \times T_A + 1.2571$). This relationship was used to calculate the inflow temperature based on the projected air temperature within each climate scenario (Fig S-A6). A similar approach can be found in Mi et al., 2020 and Bueche and Vetter (2015).

2.2.2. Model calibration and validation

The calibration period of the model was from August 26 to August 31, 2016, during the stratification period, and the verification period was from September 15, 2016, to February 15, 2017. The inflow water temperature and meteorological input data included measured data from the observational points shown in Fig. 1. We used monthly measured data from a YSI EXO2 probe, and extracted values for the calibration and verification periods for the upstream area of the dam.

The calibration of the Pangduo Reservoir CE-QUAL-W2 model focused on the shading coefficients (SHADE), the wind-sheltering coefficient (WSC), and the light extinction coefficient (EXH2O), which had the greatest influence on the simulated temperature profiles. Sensitivity analysis showed that when SHADE was set to 0.8, WSC was 1.0, and EXH2O was 0.45 m^{-1}, the generated temperature profile best matched the measured temperature profile (Fig. S-A8 and Table S-A4).

The verification period included the low-temperature period in winter and the high-temperature period in summer. Simulated and measured variations in the temperatures of the epilimnion, the metalimnion, and the hypolimnion were generally well matched (Fig. 2). The average error was 0.1 °C, the standard deviation (STD) was 0.50 °C, and the root-mean-square error (RMSE) was 0.498 °C during the entire verification period.

2.3. Statistical analysis and stratification index

To better evaluate changes in the thermal stratification and the water temperature stratified structure of. the waterbody, the buoyancy frequency (N, 1/s) (Dake and Harleman, 1969), which indicates the stability of the water column, was applied:

$$N = \sqrt{-\frac{g}{\rho_0}\frac{\partial \rho(z)}{\partial z}} \tag{1}$$

where $\rho(z)$ is the density at depth z (kg/m^3), which is assumed to be solely temperature dependent (Cole and Buchak, 2003); ρ_0 is the average density of the whole water column (kg/m^3); and g is the acceleration of gravity (m/s^2).

The stratification stability index (SI) was selected to quantify the stratification stability of the water column, which was calculated as follows (Sahoo et al., 2016):

$$SI = \int_{Z_0}^{Z_l} (Z - \overline{Z})\rho_Z dz \tag{2}$$

where Z is the depth of the water column from the surface; Z_0, Z_l, and $\overline{Z}$ are the depths of the surface water, the lower end of the water column, and the centroid of the water column, respectively; and ρ_Z is the water density at depth Z.

Water age (days) describes the duration of time that water remains in a waterbody and is defined as the persistence of water after it enters a reservoir from upstream. In CE-QUAL-W2, water age was calculated as a variable using transportation equation with the zero-order decay rate of –1 d^{-1}. As the value of inflow was set to 0 when entering the reservoir, it would increase by 1 per day if it wouldn't been diluted or discharged off from reservoir. The source term of water age in transportation equation is as follow (Cole and Buchak, 2003):

$$S_{age} = -K; \qquad K = -1/\text{day} \tag{3}$$

The temperature of the river water flowing into a reservoir is almost always different from the temperature of the surface, meaning that the density is also different. Whenever the density of the inflow waterbody is equal to the density of the reservoir waterbody, the inflow waterbody leaves the river bottom and the inflow intrudes into the reservoir horizontally. Here, the inflow intrusion depth was determined by searching the vertical water temperature in front of the dam—from the surface to the bottom—for the location where the lake temperature was equal to the inflow water temperature. The difference between the water level and the elevation at this isothermal point was adopted as the calculated intrusion depth.

Microsoft Excel 2010 was used for all statistical procedures including linear regression analysis and Mann-Kendall tests with a significance level of $|Z| > 1.96$ (Kendall, 1990; Mann, 1945).

3. Results

3.1. Thermal structure

The modeled daily vertical temperature from 2022 to 2099 upstream of the dam showed that Pangduo Reservoir is a typical dimictic

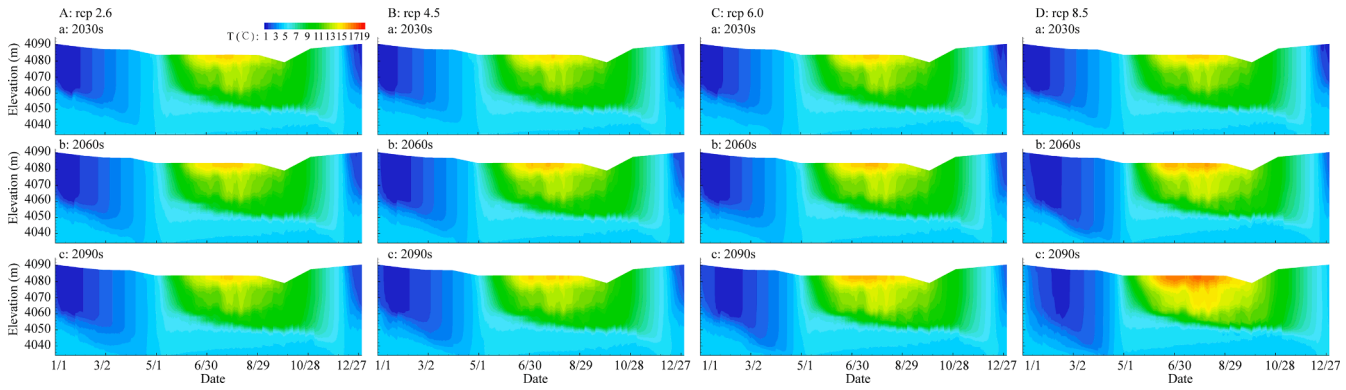

Fig. 3. Vertical water temperature variations in the 2030 s, 2060 s, and 2090 s upstream of Pangduo Dam under (A) RCP 2.6, (B) RCP 4.5, (C) RCP 6.0, and (D) RCP 8.5.

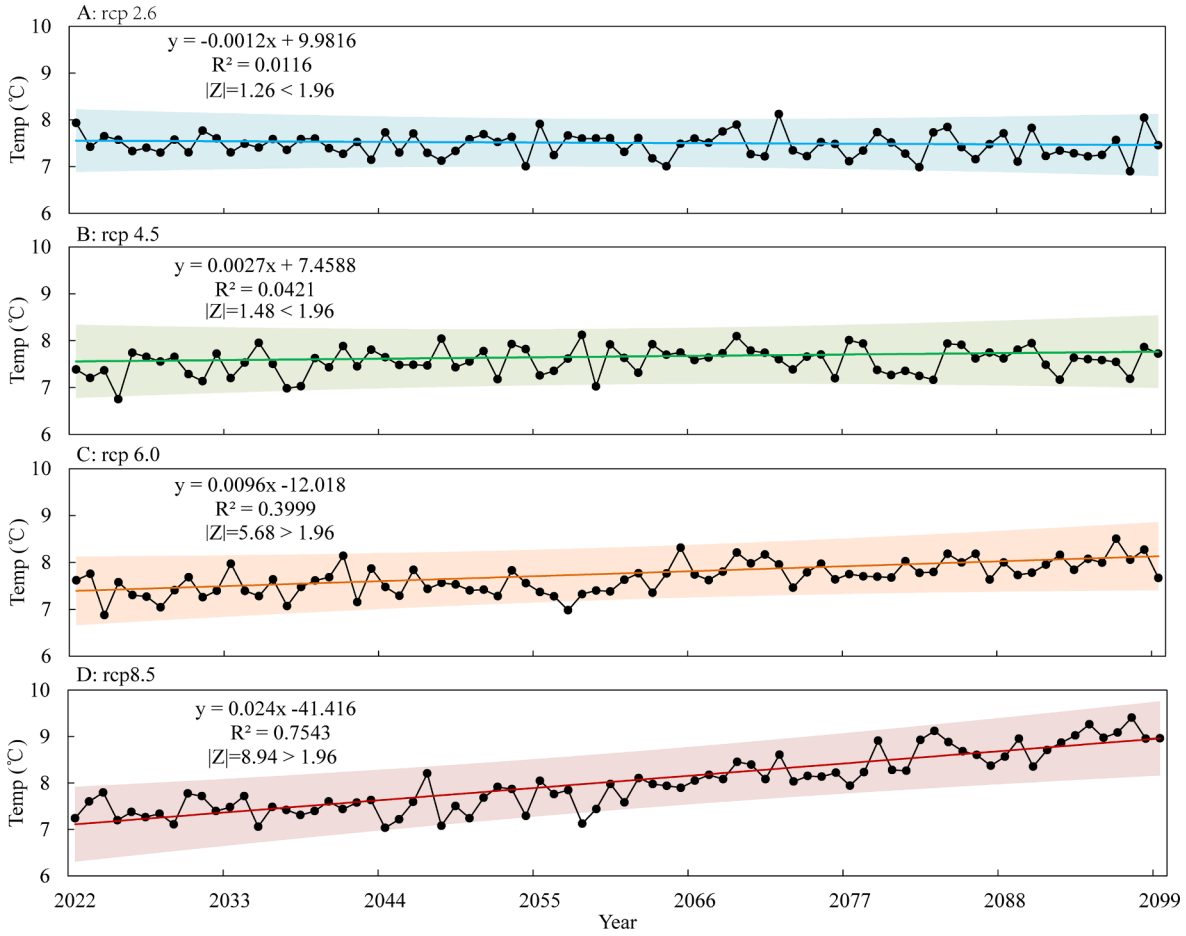

Fig. 4. Average annual surface water temperature variations from 2022 to 2099 upstream of Pangduo Dam under (A) RCP 2.6, (B) RCP 4.5, (C) RCP 6.0, and (D) RCP 8.5.

reservoir, with similar variations observed in each scenario (Fig. S-B1). The water column showed the same vertical temperature structure in April and November. In winter, the surface remains ice-covered and the bottom water temperature is stable at approximately 4 °C. In summer, the water column is thermally stratified, with higher surface water temperatures, and the thermocline mainly occurs at depths of 20–30 m. However, due to the variability of the input data, a variable inter-annual temperature structure was observed in the model. To analyze differences between each model scenario further, averaged daily data were examined decadally for the 2030s, 2060s, and 2090s (Fig. 3). The average daily surface water temperatures (under the ice during ice-covered periods) during these decades under RCP 2.6 were stable at 6.61, 6.54, and 6.50 °C, respectively, and the difference between the three typical years was<0.11 °C. However, under RCP 8.5, the average temperatures were 6.51, 7.13, and 7.85 °C, respectively, which is 1.34 °C higher in the 2090s and 2030s projections.

Upstream of the dam, between 2022 and 2099 and under the same initial field conditions, the average annual surface water temperature during the 78-year simulation period was 7.46, 7.56, 7.67, 8.00 °C under RCP 2.6, 4.5, 6.0, and 8.5, respectively (Fig. 4), with corresponding rates

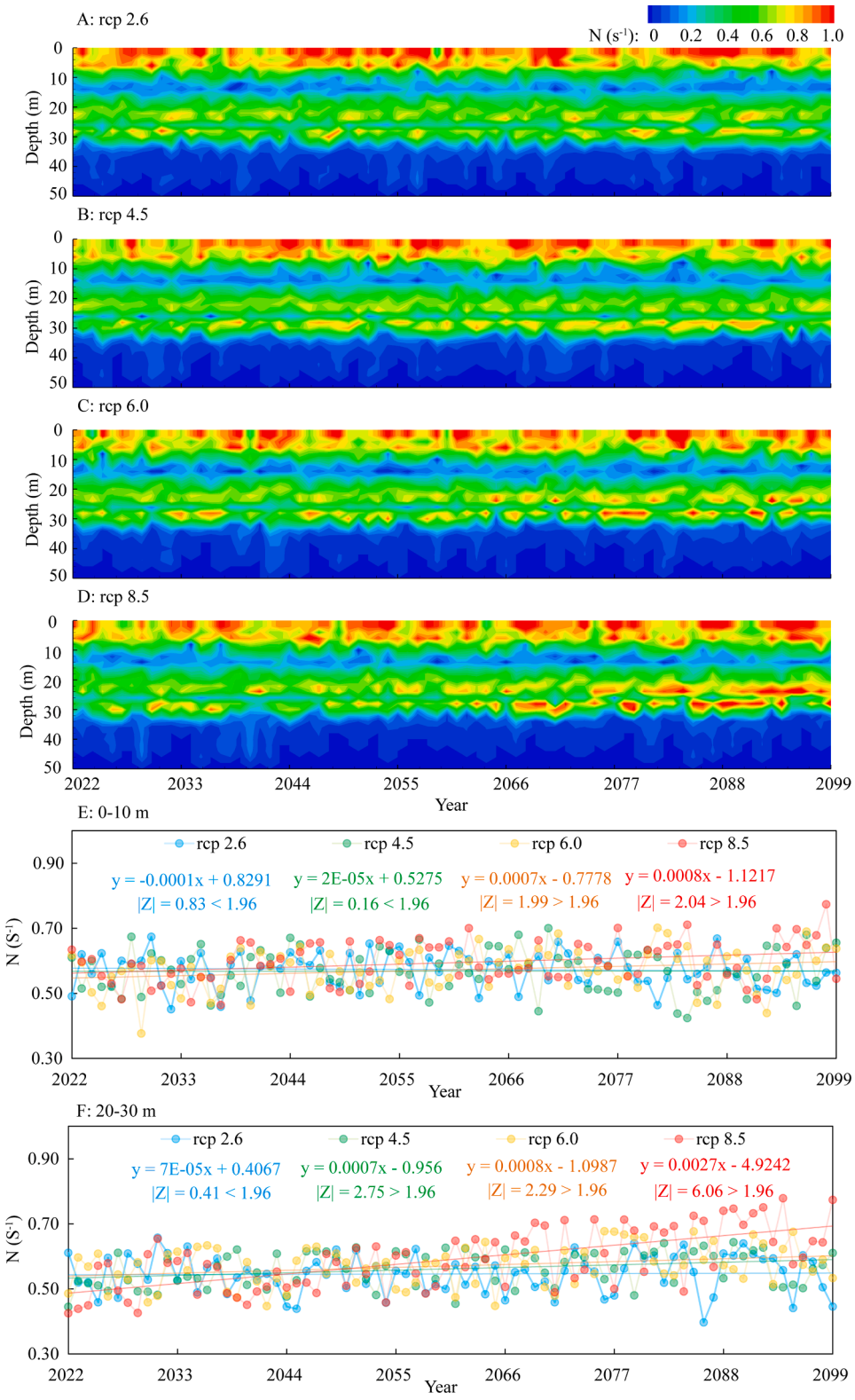

Fig. 5. Daily vertical buoyancy frequency variations from 2022 to 2099 for the day with maximum stratification upstream of Pangduo Dam under (A) RCP 2.6, (B) RCP 4.5, (C) RCP 6.0, and (D) RCP 8.5, the average buoyancy frequency at 0–10 m (E) and 20–30 m (F).

of change of 0.00, 0.05, 0.12, and 0.22 °C decade^{-1}, respectively. RCP 2.6 and 4.5 showed no significant trends ($|Z_{RCP2.6}| = 1.25 < 1.96$; $|Z_{RCP4.5}| = 1.48 < 1.96$), while the surface water temperature increased significantly under RCP 6.0 and 8.5 ($|Z_{RCP6.0}| = 5.68 > 1.96$; $|Z_{RCP8.5}| = 8.94 > 1.96$).

3.2. Reservoir stratification and stability

The daily vertical buoyancy frequency from 2022 to 2099 upstream of the dam varied between 0 and 1.2 s^{-1} in the 0–15 m zone of the epilimnion (Fig. S-B2). The average annual surface buoyancy frequency remained stable under RCP 2.6 ($|Z_{RCP2.6}| = 0.21 < 1.96$) but increased

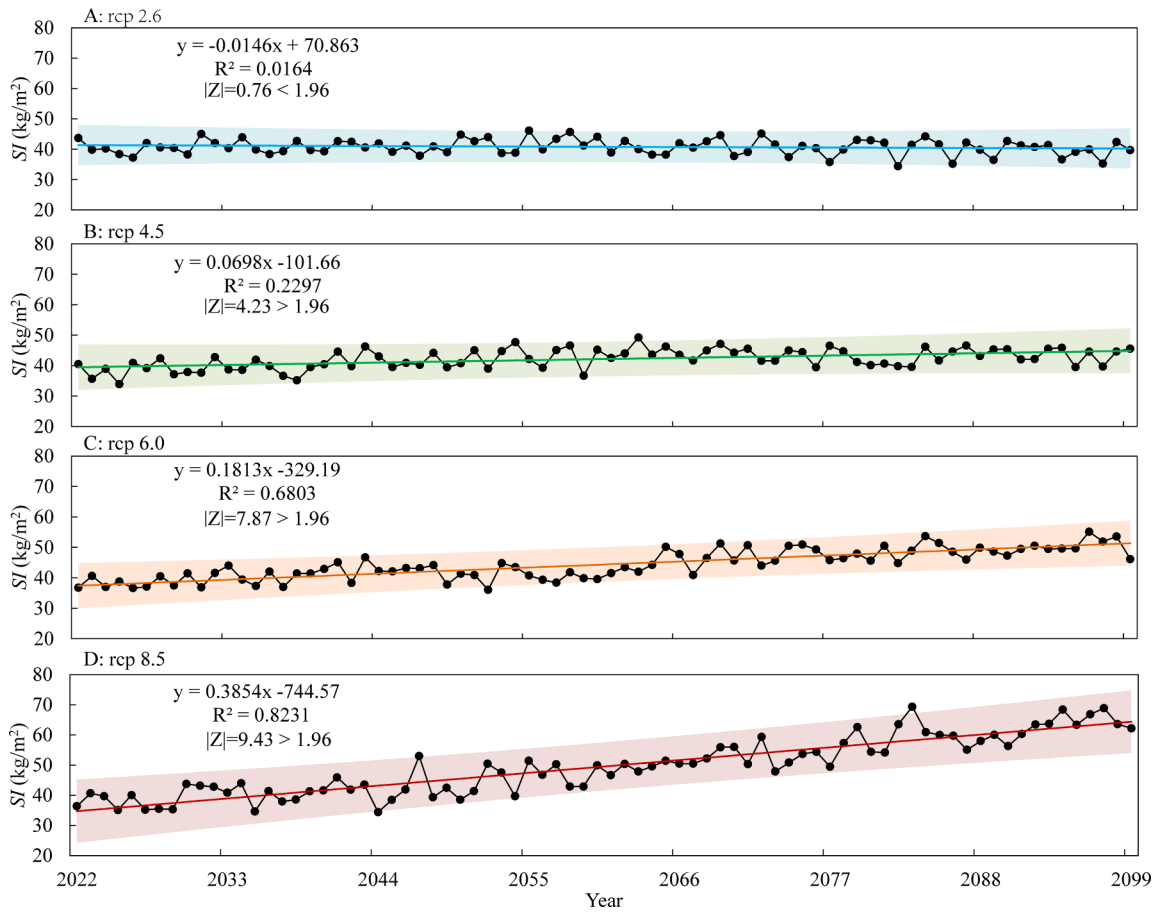

Fig. 6. Average annual SI variations from 2022 to 2099 upstream of Pangduo Dam under (A) RCP 2.6, (B) RCP 4.5, (C) RCP 6.0, and (D) RCP 8.5.

significantly under RCP 4.5 ($|Z_{RCP4.5}| = 2.04 > 1.96$), RCP 6.0 ($|Z_{RCP6.0}| = 3.05 > 1.96$), and RCP 8.5 ($|Z_{RCP8.5}| = 6.86 > 1.96$). Furthermore, the average annual buoyancy frequency in the thermocline (at depths of 20–30 m) showed significant upward trends under RCP 4.5 ($|Z_{RCP4.5}| = 3.10 > 1.96$), RCP 6.0 ($Z_{RCP6.0}| = 6.75 > 1.96$), and RCP 8.5 ($|Z_{RCP8.5}| = 9.08 > 1.96$).

The buoyancy frequency for the day with the strongest stratification in summer is shown in Fig. 5 (i.e., the largest temperature difference between the surface and bottom, with stable multi-year average dates between July 17 to July 22 under four scenarios, with no significant trends). RCP 6.0 and 8.5 showed significant upward trends ($|Z_{RCP6.0}| = 1.99 > 1.96$; $|Z_{RCP8.5}| = 2.03 > 1.96$). The average buoyancy frequency in the thermocline (at depths of 20–30 m) under each scenario was 0.55, 0.56, 0.57, and 0.60 s^{-1} under RCP 2.6, 4.5, 6.0, and 8.5, respectively, and showed significant upward trends under RCP 4.5 ($|Z_{RCP4.5}| = 2.75 > 1.96$), RCP 6.0 ($Z_{RCP6.0}| = 2.28 > 1.96$), and RCP 8.5 ($|Z_{RCP8.5}| = 6.06 > 1.96$).

Fig. 6 shows the annual average stratified stability index (*SI*) upstream of Pangduo Dam from 2022 to 2099 under the four scenarios, with values of 40.68, 42.15, 44.29, and 49.48 kg/m^2 under RCP 2.6, 4.5, 6.0, and 8.5, respectively. The annual mean *SI* increased significantly under RCP 4.5 ($|Z_{RCP4.5}| = 4.22 > 1.96$), RCP 6.0 ($|Z_{RCP6.0}| = 7.87 > 1.96$), and RCP 8.5 ($|Z_{RCP8.5}| = 9.45 > 1.96$) but was stable under RCP 2.6 ($|Z_{RCP2.6}| = 0.76 < 1.96$). Under all future scenarios, stratification stability gradually strengthened over time.

3.3. Water age

Although the water age distributions under the four scenarios were similar, there were some quantitative differences (Fig. S-B3). In spring (April) and autumn (November), the water age distribution of the water column was at approximately 160 and 55 d, respectively. In summer, due to thermal stratification, exchange between the upper and the lower waterbody was prevented and the waterbody was mainly replaced in the middle and upper water column, when the water age varied between 10 and 80 d. In the autumn, retention in the hypolimnion increased to approximately 300 d until vertical turnover occurred. Under RCP 2.6, the average water age of the hypolimnion in the 2030s, 2060s, and 2090s was 224, 225, and 225 d, respectively. In comparison, under RCP 8.5, the water age at the bottom was 224, 233, and 242 d in the 2030s, 2060s, and 2090s, respectively. In the 2090s, the average age of the hypolimnion increased by 18.6 d relative to the 2030s (Fig. S-B4).

Fig. 7 shows the average annual water age at the bottom (considered the lowest cell) upstream of the dam under each scenario from 2022 to 2099. With the same initial conditions, the average age of the bottom water over the 78-year simulation period was 224, 226, 228, and 232 d under RCP 2.6, 4.5, 6.0, and 8.5, respectively, with significant corresponding trends of 0.05 ($|Z_{RCP2.6}| = 2.31 > 1.96$), 0.92 ($|Z_{RCP4.5}| = 3.62 > 1.96$), 1.73 ($|Z_{RCP6.0}| = 7.68 > 1.96$), and 3.2 d $decade^{-1}$ ($|Z_{RCP8.5}| = 9.40 > 1.96$). These trends indicate that the bottom water remained in place for a progressively longer period and, as such, became increasingly difficult to replace with new water.

4. Discussion

4.1. Response of the dimictic reservoir to climate warming

The temperature structure and stratification of Pangduo Reservoir showed strong seasonal changes (Fig. 3 and Fig. 4). During the year, there was ice cover from December to March, and the reservoir was

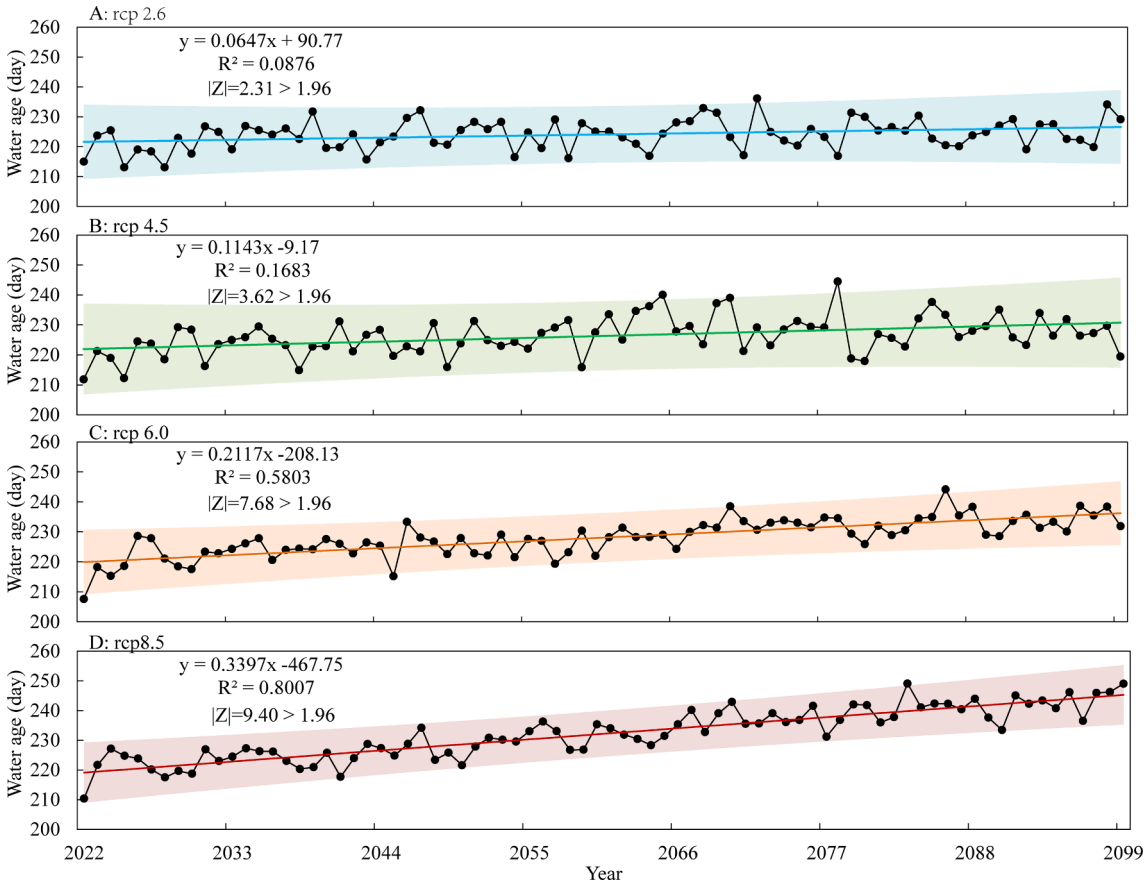

Fig. 7. Average annual water age variations from 2022 to 2099 upstream of Pangduo Dam under (A) RCP 2.6, (B) RCP 4.5, (C) RCP 6.0, and (D) RCP 8.5.

stably stratified during the rest of the year with two periods of mixing. In our analyses, we used a temperature difference of 2 °C from the surface to bottom to indicate stratification. Under each scenario, from late November to early December, air temperatures were below 0 °C, the heat loss rate from the reservoir accelerated, and the surface water temperature cooled and convective sinking occurred. The temperature structure tended towards a vertically isothermal structure until the temperature fell to 3.94 °C, and the further loss of heat in the surface waterbody caused a vertical temperature gradient inversion. This structure remained stable under RCP 2.6 but showed delays of 1.1, 1.8, and 4.1 d decade^{-1} under RCP 4.5, 6.0, and 8.5, respectively. When ice formed at the surface, the ice layer provided thermal protection for the waterbody such that heat exchange shifted from water-to-air to ice-to-water heat exchange. This ice-layer protection mechanism results in a relatively stable waterbody, and the temperature inversion is delayed accordingly (Öğlü et al., 2020). Until the freezing period is over, more than half of the solar energy is absorbed by the upper layers. This absorbed heat is no longer used to melt ice-cover, and the heat budget of the surface waterbody is controlled by penetrating short-wave radiation and cooling via surface heat loss (Li et al., 2018; Wang et al., 2020). The snow-cover was not considered in this study, because the study area was mostly in the temperate monsoon climate zone, and the average precipitation was only 2 mm per month in winter from 1981 to 2010. During the 78-year simulation period, under RCP 2.6, 4.5 and 6.0, climate warming was not sufficient to change the freezing state in winter, but in the 2080s to 2090s, there were some years without ice cover under the rcp85 scenario (Fig. S-B5). In conditions without ice-cover, the surface water temperature rose and the temperature inversion stratification could disappear. The ice thickness was significantly reduced under RCP 4.5 ($|Z_{RCP4.5}| = 5.00 > 1.96$), RCP 6.0 ($|Z_{RCP6.0}| = 5.17 > 1.96$), and RCP 8.5 ($|Z_{RCP8.5}| = 8.44 > 1.96$). At the same time, the number of ice-covered days in winter reduced under RCP 4.5 ($|Z_{RCP4.5}| = 5.70 > 1.96$), RCP 6.0 ($|Z_{RCP6.0}| = 5.28 > 1.96$), and RCP 8.5 ($|Z_{RCP8.5}| = 8.79 > 1.96$), which is consistent with existing studies (Woolway and Merchant, 2019).

Reservoirs typically control larger catchment areas and have more inflows than natural lakes, and their catchment areas often show a stronger degree of interaction and greater momentum (Hayes et al., 2017). The outlet structure is an important component of many reservoirs (Naderi et al., 2014), having an overall effect on the waterbody and, therefore, generating areas of dominant flows (Akiyama and Stefan, 1987). For example, higher flow rates and the existence of interflow often enhance water mixing and lower water ages compared to lakes (Hayes et al., 2017). In Pangduo Reservoir, the heat of inflow during the warming period is not stored in the waterbody but released through the interflow with discharged water. The inflows to lakes are quickly mixed and stagnate for longer than in reservoirs, accumulating heat more effectively. While summer thermal stratification in Erken Lake and Nam Co Lake has advanced from 4 d to 3 weeks (Arvola et al., 2009; Huang et al., 2017), we observed that this was postponed by 0.2 to 6.9 d in Pangduo Reservoir (Fig. 8). In summer, the heat absorption of waterbodies is higher than the heat emission, such that surface water is continuously heated. As a result, the surface water temperature rise much faster than in the deep layers. Meanwhile, combined with the effect of interflow and the light extinction of the reservoir, the thermocline can appear on the surface and the buoyancy frequency increases, which block the vertical exchange of material and energy (Zhang et al., 2014). In our simulations, the end of the summer stratification was significantly postponed by 1.17 and 3.21 d decade^{-1} under RCP 6.0 ($|Z_{RCP6.0}| = 1.99 > 1.96$) and RCP 8.5 ($|Z_{RCP8.5}| = 6.93 > 1.96$), respectively, but remained stable under RCP 2.6 ($|Z_{RCP2.6}| = 0.42 < 1.96$) and RCP 4.5 ($|Z_{RCP4.5}| = 0.28 < 1.96$) (Fig. 8 and Fig. S-B6). There

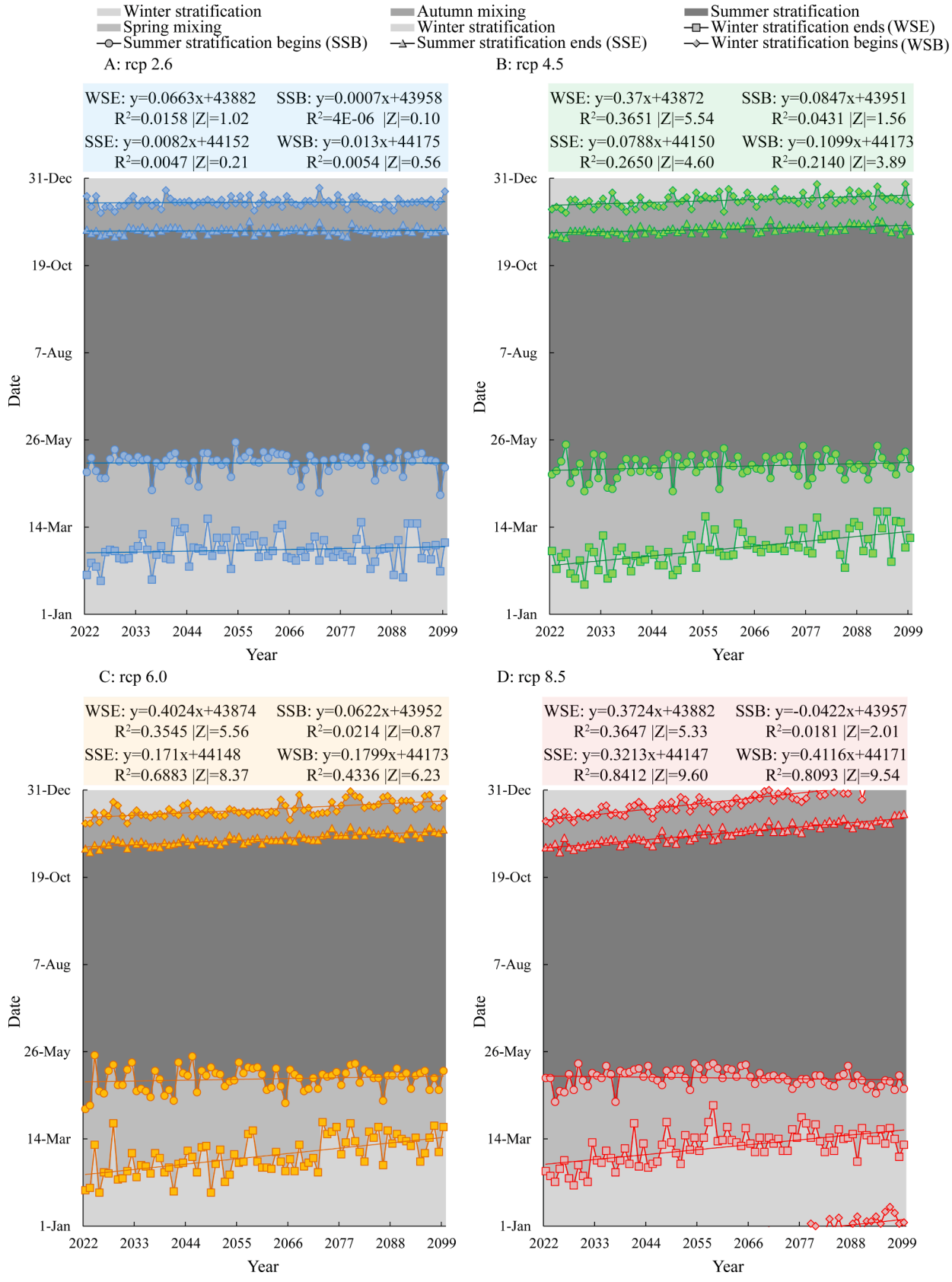

Fig. 8. Variations in the start of winter stratification, the end of winter stratification, the beginning of summer stratification, and the end of summer stratification in Pangduo Reservoir from 2022 to 2099 under (A) RCP 2.6, (B) RCP 4.5, (C) RCP 6.0, and (D) RCP 8.5. (The significance level of Mann-Kendall test is $|Z| > 1.96$).

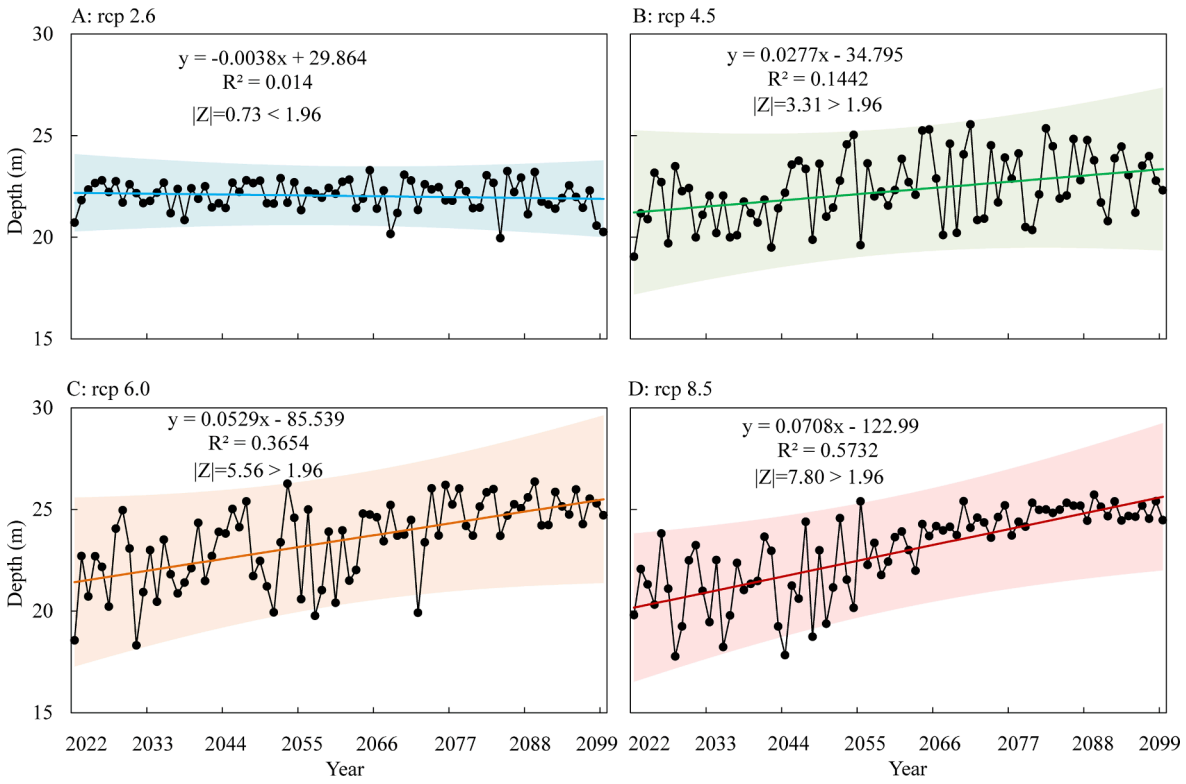

Fig. 9. Average annual inflow intrusion depth variations from 2022 to 2099 under (A) RCP 2.6, (B) RCP 4.5, (C) RCP 6.0, and (D) RCP 8.5.

was a long period of stratification in summer after the mixing in spring. Therefore, the spring mixing period is a particularly important DO supplementation process. The spring mixing period remained stable under RCP 2.6, which significantly decreased by 2.85, 3.40, and 4.1 d decade^{-1} under RCP 4.5 ($|Z_{RCP4.5}| = 4.81 > 1.96$), RCP 6.0 ($|Z_{RCP6.0}| = 5.56 > 1.96$), and RCP 8.5 ($|Z_{RCP8.5}| = 6.02 > 1.96$), respectively (Fig. S-B7). The thermal stratification of lakes and reservoirs may cause a series of environmental impacts, especially in the case of DO (North et al., 2014). Previous studies show that an increase in the duration of thermal stratification in summer increases the duration of hypoxic conditions in the bottom water (Foley et al., 2011).

In our modeling, we used a buoyancy frequency of 0.2 s^{-1} as the threshold value of the average annual thickness of the metalimnion. Under the four climate scenarios, the upper boundary of the metalimnion advanced toward the surface by 0.10–0.59 m over the 78-year simulation period, while the lower boundary remained relatively stable (average thickness range = 0.12–0.43 m). However, the degree of stratification was not affected by this expansion of the metalimnion (Fig. S-B8), whereas buoyancy was gradually strengthened (Fig. 5).

For dimictic reservoirs at high altitudes, thermal protection during the frozen period and heat loss due to water withdrawal prevent efficient heat accumulation, which delays the vertical inversion temperature period. Furthermore, the shortening in the spring mixing period poses a potential risk for water quality. Finally, our model shows the existence of a surface thermocline in summer that block vertical exchanges in the water column and delays stratification.

4.2. Mixing characteristics in response to climate change

An important feature of run-of-river reservoirs that distinguishes them from lakes is that inflows and outflows are the main driving forces of internal mixing (Chen et al., 2016). Inflows push static water in front until the density is equalized, forming a dominant layer of intrusion water (Yildirim and Kocabaş, 1998). This delivers important nutrients for biogeochemical cycling including carbon and nitrogen (Becker et al., 2010). In Pangduo Reservoir, the inflow intrusion depth was stable during the summer stratification period under RCP 2.6 but significantly increased by 0.28, 0.53, and 0.71 m decade^{-1} under RCP 4.5 ($|Z_{RCP4.5}| = 3.31 > 1.96$), RCP 6.0 ($|Z_{RCP6.0}| = 5.56 > 1.96$), and RCP 8.5 ($|Z_{RCP8.5}| = 7.80 > 1.96$), respectively (Fig. 9). The invading flow drove nutrients to deeper areas of the reservoir. Under more intense simulated climate warming, the correlation between the inflow intrusion depth and the *SI* strengthened and, except for RCP 2.6, was significant ($R^2 = 0.18$, 0.50, and 0.75 under RCP 4.5, 6.0, and 8.5, respectively; $p < 0.01$) (Fig. 10).

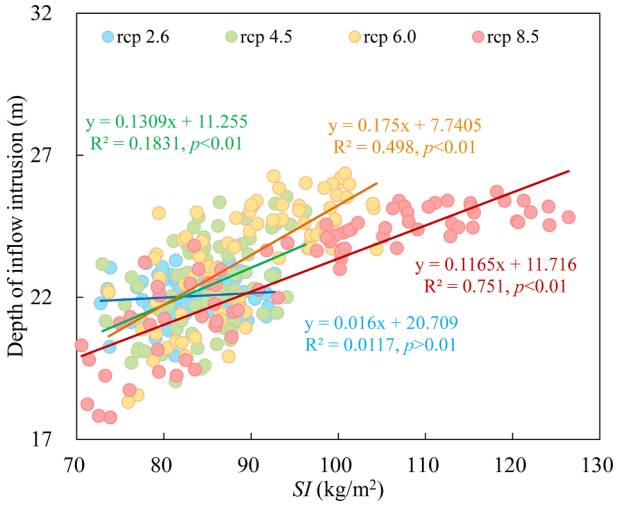

Fig. 10. Linear correlation between the intrusion depth and stratification stability intensity (SI) in Pangduo Reservoir during the summer stratification period from 2022 to 2099.

These trends indicate that strengthened thermal stratification under warming conditions would dominate the mixing characteristics of the deeper inflow intrusion in the reservoir. At the same time, due to the

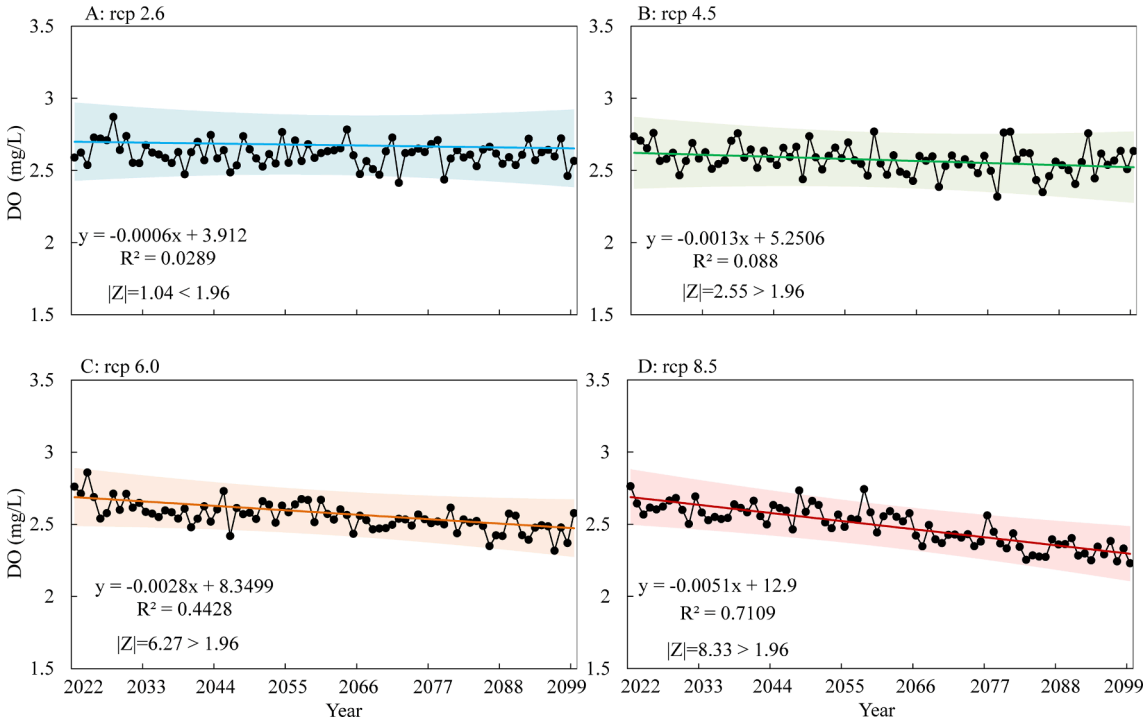

Fig. 11. Variations of DO concentrations in the hypolimnion from 2022 to 2099 under (A) RCP 2.6, (B) RCP 4.5, (C) RCP 6.0, and (D) RCP 8.5.

extension of the summer stratification period (Fig. S-B6) and the increase in water age (Fig. 7), nutrients would remain in the middle and bottom layers of the reservoir for a longer period. As long as the respiration rates of organisms in the hypolimnion are moderate, under these conditions, a waterbody would likely enter a hypoxic or even hypoxic state, which could promote the release of endogenous phosphorus in the bottom waters (North et al., 2014).

4.3. Effects of climate change on dissolved oxygen

Under climate warming, oxygen consumption in the hypolimnion during the stratification period is increased in lakes and reservoirs (Zhang et al., 2014), and altered stratification characteristics may further affect the DO regime in bottom waters. Furthermore, organic matter in the upper layer sinks to the lower layers via a series of decomposition processes that reduce the DO content (Kraemer et al., 2017). In Pangduo Reservoir, summertime DO in the epilimnion and metalimnion ranged between 5.7 and 6.5 mg/L (between 84.1 % and 95.9 % saturation) (Fig. S-B9) and was significantly depleted in the hypolimnion forming a hypoxic zone (DO $\leq$ 4 mg/L). For deep freshwater lakes and reservoirs with seasonal stratification and mixing, vertical mixing after stratification is an important and effective mechanism of DO replenishment in the hypolimnion (Sahoo et al., 2013). In Pangduo Reservoir, two periods of vertical mixing were identified, in spring and autumn; in November, before winter freezing, and in April, before the summer stratification period, the reservoir was enriched in DO (average = 7.1 mg/L).

Here we set up a discussion scenario and performed a rough calculation of the variation trends of DO. The oxygen consumption rate of the stagnant layer during the summer stratification period was 0.0125 mg/L d^{-1}, calculated according to equation (4) as follows.

$$v_{DO} = \frac{C_{DO_1} - C_{DO_2}}{\Delta t} \quad (4)$$

Where C_{DO1} and C_{DO2} were the measured DO concentrations in April and November 2017, respectively, and $\triangle t$ was the interval time. Assuming that the oxygen consumption rate is constant, we estimated the DO concentrations in the hypolimnion at the end of the stratification under the four climate scenarios (Fig. 11). The DO concentration in the hypolimnion significantly decreases under RCP 4.5, 6.0, and 8.5, being most prominent in deep reservoirs as decomposition can continue for longer before all the organic matter is consumed. Moreover, the period of hypoxia (DO $\leq$ 4 mg/L) in the hypolimnion increased significantly under RCP 2.6 and 8.5 (Fig. S-B10). Once the DO concentration in the hypolimnion exceeds the accumulation and replenishment rate of oxygen (Ito and Momii, 2015), an anaerobic environment can form, which might indirectly lead to the release of soluble endogenous phosphorus (North et al., 2014), and, furthermore, anaerobic zones are inefficient at retaining phosphorus (Garnier et al., 2005). We consider these outcomes are based on conservative estimates. Indeed, under the current warming trend, the biochemical activity in the reservoir and the oxygen consumption rate of the hypolimnion will likely increase.

Under projected climate warming, our simulations indicate that the metalimnion in Pangduo Reservoir will expand slightly and become strengthened, hindering the vertical mixing of the water column. Compression of the spring mixing period and strengthening of summer stratification will likely greatly weaken the mechanism by which DO is supplemented to the hypolimnion through vertical mixing. As long as the lake stays dimictic, the DO supply mechanism would not be completely destroyed. Hypoxia in the hypolimnion during the summer stratification period is, therefore, enhanced. Additionally, we expect the inflow intrusion depth to significantly increase under furture climate warming scenarios, with thermal stratification further dominating the mixing characteristics in the reservoir. Finally, based on the supply and retention of nutrients in the bottom waters, the accumulation of organic matter and the consumption of oxygen in the hypolimnion are promoted, which could further threaten water quality.

4.4. Future perspectives

Changes in thermal mixing regimes of reservoirs under climate warming threaten water quality security and biodiversity (Walsh et al., 2020). As primary drinking water resources, effective reservoir management must balance economic goals and environmental protection

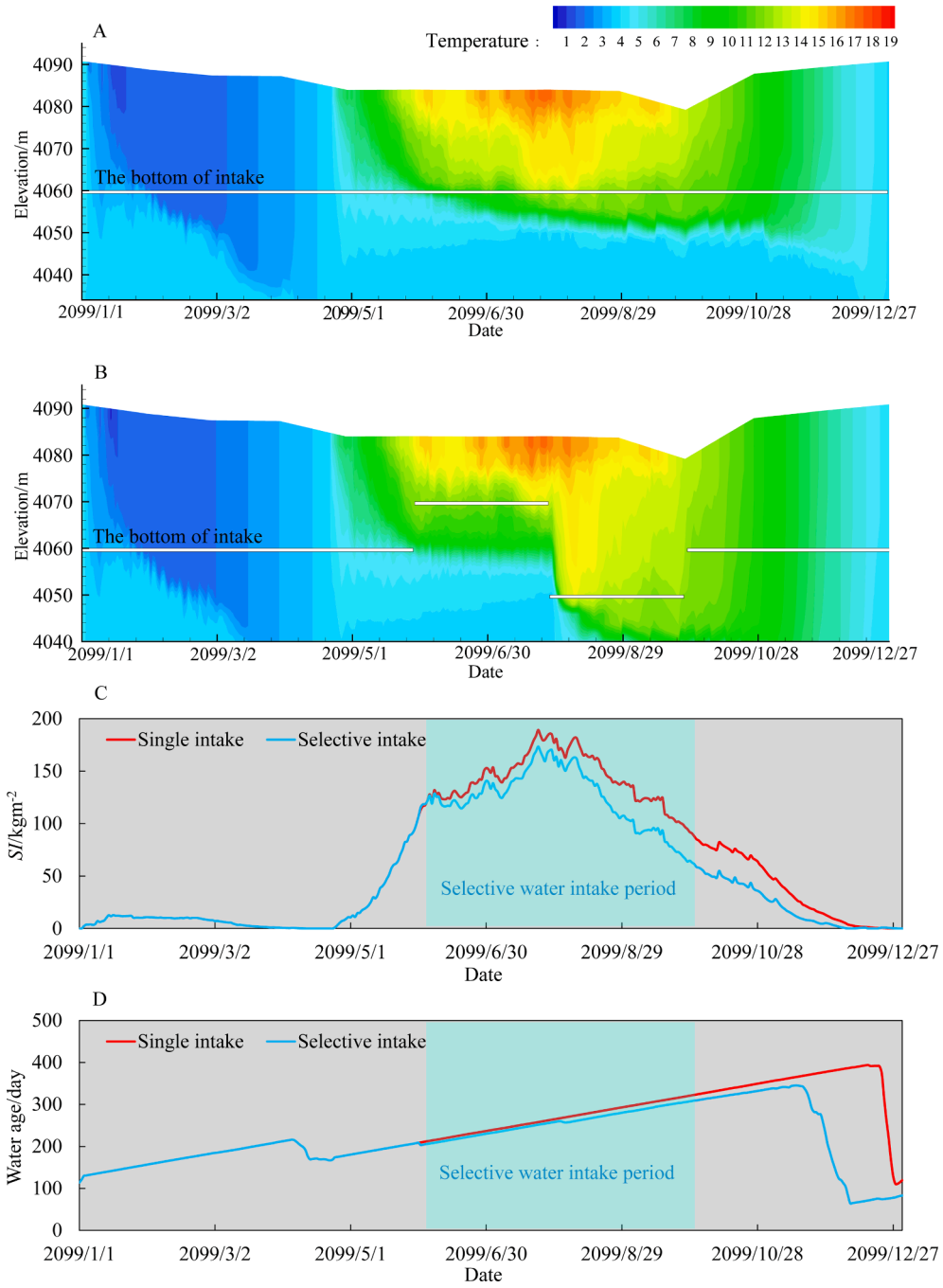

Fig. 12. The comparison of the selective water intake and the single water intake in Pangdo in 2099 under RCP 8.5, A. vertical temperature variations of single intake case; B. vertical temperature variations of selective intake case; C. comparison of the SI time series of selective and single intake cases; D. comparison of the water age time series of selective and single intake cases.

requirements (Weber et al., 2017). In many reservoirs in the temperate North, utilizing taking water from the hypolimnion is a fundamental strategy. This aims to enhance vertical mixing, avoid hypoxia, and reduce the release of nutrients from sediment (Çalışkan and Elçi, 2009). As such, the selective water intake mode of reservoirs is an important management model to control thermal regimes both the reservoir areas and downstream rivers. This is mainly achieved by drawing water from the epilimnion and metalimnion to adjust the thermal regime in the reservoir area (Hallnan et al., 2020; Mi et al., 2019).

For Pangduo Reservoir, in summer, selective water extraction could be adopted to release water from the epilimnion and the upper part of the metalimnion to increase the height of the thermocline and inflow intrusion and, thereby, dilute the density differences in the upper layers. At the end of summer stratification period or earlier, releasing water from the hypolimnion would strengthen vertical mixing, accelerate the replacement of bottom water, and supplement the DO supply in autumn. For illustration, taking 2099 under RCP 8.5 scenario as an example, we considered the effect of taking water from the epilimnion from June to July, and from August to July from the hypolimnion (Fig. 12) (Pangduo Reservoir did not actually have selective water intakes, and here was only a design discussion condition). Based on June to September water-intake test period, the average *SI* was 141.78 kg/m^2 (single intake case) and 123.03 kg/m^2 (selective intake case), respectively, the stratification strength of the selective intake case was reduced by 13.2 %. This effect

would continue into winter. The average water age of bottom water was 266.14 d (single intake case) and 256.50 d (selective intake case), respectively. Due to the delay in the flow in the reservoir, it would be easier to replace the water at the hypolimnion during the cooling period (November) after the stratification is weakened. However, it should be noted that thermal stratification is controlled by a range of factors encompassing climatic conditions, reservoir operation modes, and water intake locations as well as operational safety and economic constraints (Song et al., 2019). Further research is needed, therefore, to examine the individual and combined influences of these different factors.

Previous studies indicate that reservoirs undergo a subtle mixing process over diurnal cycles (Yang et al., 2020). Specifically, the epilimnion is heated during the day and cools at night. Consequently, heat flux from surface layers fluctuates positively and negatively throughout the day, and vertical density convection can occur (Van Emmerik et al., 2013). Such convective movement promotes the mixing of upper layers of water, which generally erodes the stable thermocline structure and can weaken the buoyancy effect during the summer stratification period (Vercauteren et al., 2011). Future research is now required to consider the impacts of such diurnal thermal regimes in reservoirs, especially with respect to the response of mixing mechanisms to climate change.

5. Conclusions

A two-dimensional hydrodynamic model (CE-QUAL-W2) was configured to study the response of thermal and mixing regimes to climate change in the dimictic Pangduo Reservoir on the QTP. Based on our results, a delay in summer stratification was a key response, corresponding to an extension of 1.17 and 3.21 d decade^{-1} under RCP 6.0 and 8.5, respectively. The spring mixing period showed significant compression, reducing by 2.85, 3.40, and 4.10 d decade^{-1} under RCP 4.5, 6.0, and 8.5, respectively. This is a potential threat to oxygen replenishment in spring.

Under the studied climate warming scenarios, the metalimnion expanded slightly while its stratification strength increased, preventing vertical mixing in the water column. Moreover, the depth of inflow penetration increased significantly by 0.28, 0.53, and 0.71 m decade^{-1} under RCP 4.5, 6.0, and 8.5, respectively. This was associated with enhanced thermal stratification. The increase in the inflow intrusion depth and the extension of the retention time of the hypolimnion are potential risks to water quality in this region. The DO concentrations in the hypolimnion also significantly decreased under RCP 4.5, 6.0, and 8.5. Overall, our results provide valuable new evidence to help support the development of appropriate adaptive management strategies for Pangduo Reservoir as well as similar dimictic reservoirs in other high-altitude regions.

CRediT authorship contribution statement

Yanjing Yang: Conceptualization, Data curation, Investigation, Methodology, Writing – original draft, Writing – review & editing, Software. **Min Chen:** Conceptualization, Data curation, Funding acquisition, Project administration, Software, Supervision, Validation, Writing – review & editing. **Yun Deng:** Investigation, Project administration, Methodology, Validation. **S. Geoffrey Schladow:** Conceptualization, Methodology, Writing – review & editing. **Jia Li:** Supervision, Project administration, Validation. **You-Cai Tuo:** Investigation, Software.

Declaration of Competing Interest

The authors declare that they have no known competing financial interests or personal relationships that could have appeared to influence the work reported in this paper.

Acknowledgments

Funding: This project was supported by the National Natural Science Foundation of China [Grant No. 51909176], China.

Appendix A. Supplementary data

Supplementary data to this article can be found online at https://doi.org/10.1016/j.jhydrol.2021.127141.

References

Akiyama, J., Stefan, H.G., 1987. Gravity Currents in Lakes. Two-Layer Stratified Flow Analysis. St Anthony Falls Laboratory, Reservoirs and Coastal Regions.
Arvola, L., George, G., Livingstone, D.M., Jrvinen, M., Weyhenmeyer, G.A., 2009. The Impact of the Changing Climate on the Thermal Characteristics of Lakes. Springer, Netherlands.
Becker, V., Caputo, L., Ordóñez, J., Marcé, R., Armengol, J., Crossetti, L.O., Huszar, V.L. M., 2010. Driving factors of the phytoplankton functional groups in a deep Mediterranean reservoir. Water Res. 44 (11), 3345–3354.
Bueche, T., Vetter, M., 2015. Future alterations of thermal characteristics in a mediumsized lake simulated by coupling a regional climate model with a lake model. Clim. Dyn. 44 (1-2), 371–384.
Foley, B., Jones, I.D., Maberly, S.C., Rippey, B., 2011. Long-term changes in oxygen depletion in a small temperate lake: effects of climate change and eutrophication. Freshwater Biol. 57 (2), 278–289.
Caldwell, T.J., Chandra, S., Feher, K., Simmons, J.B., Hogan, Z., 2020. Ecosystem response to earlier ice break-up date: Climate-driven changes to water temperature, lake-habitat-specific production, and trout habitat and resource use. Glob. Change Biol. 26 (10), 5475–5491.
Çalışkan, A., Elçi, Ş., 2009. Effects of Selective Withdrawal on Hydrodynamics of a Stratified Reservoir. Water Resour. Manag. 23 (7), 1257–1273.
Chen, G., Fang, X., 2015. Sensitivity Analysis of Flow and Temperature Distributions of Density Currents in a River-Reservoir System under Upstream Releases with Different Durations. Water-Sui. 7 (11), 6244–6268.
Cole, T.M., Buchak, E.M., 2003. CE-QUAL-W2: A Two-Dimensional, Laterally Averaged, Hydrodynamic and Water Quality Model, Version 2.0. User Manual. Civil and Environmental Engineering Faculty Publications and Presentations.
Czernecki, B., Ptak, M., 2018. The impact of global warming on lake surface water temperature in Poland - the application of empirical-statistical downscaling, 1971–2100. J. Limnol. 77 (2).
Dake, J.M.K., Harleman, D.R.F., 1969. Thermal stratification in lakes: Analytical and laboratory studies. Water Resour. Res. 5 (2), 484–495.
Ding, YongJian, Ye, BaiSheng, Han, TianDing, Shen, YongPing, Liu, ShiYin, 2007. Regional difference of annual precipitation and discharge variation over west China during the last 50 years. Sci. China 50 (6), 936–945.
Frieler, K., Lange, S., Piontek, F., Reyer, C.P., Schewe, J., Warszawski, L., Zhao, F., Chini, L., Denvil, S., Emanuel, K., 2017. Assessing the impacts of 1.5 °C global warming-simulation protocol of the Inter-Sectoral Impact Model Intercomparison Project (ISIMIP2b). Geosci. Model Dev. 10, 4321–4345.
Chen, G., Fang, X., Devkota, J., 2016. Understanding flow dynamics and density currents in a river-reservoir system under upstream reservoir releases. Hydrological Sciences Journal/journal Des Sciences Hydrologiques 61 (13), 2411–2426.
Garnier, J., Némery, J., Billen, G., Théry, S., 2005. Nutrient dynamics and control of eutrophication in the Marne River system: modelling the role of exchangeable phosphorus. J. Hydrol. 304 (1-4), 397–412.
Hallnan, R., Saito, L., Busby, D., Tyler, S., 2020. Modeling Shasta Reservoir Water-Temperature Response to the 2015 Drought and Response under Future Climate Change. J. Water Res Plan. Man. 146 (5), 04020018. https://doi.org/10.1061/(ASCE)WR.1943-5452.0001186.
Hayes, N.M., Deemer, B.R., Corman, J.R., Razavi, N.R., Strock, K.E., 2017. Key differences between lakes and reservoirs modify climate signals: A case for a new conceptual model. Limnol. Oceanogr. Lett. 2 (2), 47–62.
He, W., Lian, J., Zhang, J., Yu, X., Chen, S., 2019. Impact of intra-annual runoff uniformity and global warming on the thermal regime of a large reservoir. Sci. Total Environ. 658, 1085–1097.
Huang, L., Wang, J., Zhu, L., Ju, J., Daut, G., 2017. The Warming of Large Lakes on the Tibetan Plateau: Evidence From a Lake Model Simulation of Nam Co, China, During 1979–2012. J. Geophys. Res. [Atmos.] 122 (24), 13,095–13,107.
Ito, Y., Momii, K., 2015. Impacts of regional warming on long-term hypolimnetic anoxia and dissolved oxygen concentration in a deep lake. Hydrol. Process. 29 (9), 2232–2242.
Kendall, M.G., 1990. Rank Correlation Methods. Brit. J. Psychol. 25 (1), 86–91.
Kraemer, B.M., Chandra, S., Dell, A.I., Dix, M., Kuusisto, E., Livingstone, D.M., Schladow, S.G., Silow, E., Sitoki, L.M., Tamatamah, R., McIntyre, P.B., 2017. Global patterns in lake ecosystem responses to warming based on the temperature dependence of metabolism. Glob. Change Biol. 23 (5), 1881–1890.
Lange, S., 2017. Bias correction of surface downwelling longwave and shortwave radiation for the EWEMBI dataset. Earth Syst. Dynam. Discuss. 9 (2), 1–30.
Lewis, W.M., McCutchan, J.H., Roberson, J., 2019. Effects of Climatic Change on Temperature and Thermal Structure of a Mountain Reservoir. Water Resour. Res. 55 (3), 1988–1999.

Li, F., Jiang, X.u., Cui, C., 2020. Thermal structure and response on local climate and hydrological changes in a reservoir with an icebound season. J. Hydro-environ. Res. 31, 48–61.
Li, N., Tuo, Y.-C., Deng, Y., An, R.-D., Li, J., Liang, R.-F., 2018. Modeling of thermodynamics of ice and water in seasonal ice-covered reservoir. J. Hydrodyn. 30 (2), 267–275.
Magee, M.R., Wu, C.H., 2017. Response of water temperatures and stratification to changing climate in three lakes with different morphometry. Hydrol. Earth Syst. Sci. Discuss. 21 (12), 1–40.
Mann, H.B., 1945. Nonparametric test against trend. Econometrica 13 (3), 245–259.
Mengzhen, X., Zhaoyin, W., Baozhu, P., Tongliang, G., Le, L., 2012. Research on assemblage characteristics of macroinvertebrates in the Yalu Tsangpo River Basin. Acta Ecol. Sin. 32 (8), 2351–2360.
Mi, C., Sadeghian, A., Lindenschmidt, K.-E., Rinke, K., 2019. Variable withdrawal elevations as a management tool to counter the effects of climate warming in Germany's largest drinking water reservoir. Environ. Sci. Europe 31 (1), 19.
Mi, C., Shatwell, T., Ma, J., Xu, Y., Su, F., Rinke, K., 2020. Ensemble warming projections in Germany's largest drinking water reservoir and potential adaptation strategies. Sci. Total Environ. 748, 141366. https://doi.org/10.1016/j.scitotenv.2020.141366.
Naderi, V., Farsadizadeh, D., Hosseinzadeh Dalir, A., Arvanaghi, H., 2014. Effect of Using Vertical Plates on Vertical Intake on Discharge Coefficient. Arab. J. Sci. Eng. 39 (12), 8627–8633.
North, R.P., North, R.L., Livingstone, D.M., Köster, O., Kipfer, R., 2014. Long-term changes in hypoxia and soluble reactive phosphorus in the hypolimnion of a large temperate lake: consequences of a climate regime shift. Glob. Change Biol. 20 (3), 811–823.
Öğlü, B., Möls, T., Kaart, T., Cremona, F., Kangur, K., 2020. Parameterization of surface water temperature and long-term trends in Europe's fourth largest lake shows recent and rapid warming in winter. Limnologica 82, 125777. https://doi.org/10.1016/j.limno.2020.125777.
Piccolroaz, S., Healey, N.C., Lenters, J.D., Schladow, S.G., Hook, S.J., Sahoo, G.B., Toffolon, M., 2018. On the predictability of lake surface temperature using air temperature in a changing climate: A case study for Lake Tahoe (U.S.A.). Limnol. Oceanogr. 63 (1), 243–261.
Piccolroaz, S., Woolway, R.I., Merchant, C.J., 2020. Global reconstruction of twentieth century lake surface water temperature reveals different warming trends depending on the climatic zone. Clim. Change 160 (3), 427–442.
Ptak, M., Sojka, M., Nowak, B., 2020. Effect of climate warming on a change in thermal and ice conditions in the largest lake in Poland – Lake Śniardwy. J. Hydrol. Hydromech. 68 (3), 260–270.
Qiu, J., 2008. China: The third pole. Nature 454 (7203), 393–396.
Rogora, M., Buzzi, F., Dresti, C., Leoni, B., Lepori, F., Mosello, R., Patelli, M., Salmaso, N., 2018. Climatic effects on vertical mixing and deep-water oxygen content in the subalpine lakes in Italy. Hydrobiologia 824 (1), 33–50.
Sahoo, G.B., Forrest, A.L., Schladow, S.G., Reuter, J.E., Coats, R., Dettinger, M., 2016. Climate change impacts on lake thermal dynamics and ecosystem vulnerabilities. Limnol. Oceanog. 61 (2), 496–507.
Sahoo, G.B., Schladow, S.G., Reuter, J.E., Coats, R., Dettinger, M., Riverson, J., Wolfe, B., Costa-Cabral, M., 2013. The response of Lake Tahoe to climate change. Clim. Change 116 (1), 71–95.
Schwefel, R., Gaudard, A., Wüest, A., Bouffard, D., 2016. Effects of climate change on deepwater oxygen and winter mixing in a deep lake (Lake Geneva): Comparing observational findings and modeling. Water Resour. Res. 52 (11), 8811–8826.
Song, Q., Sun, B., Gao, X., Zhang, C., 2019. PIV experimental investigation of the outflow temperature from nonlinearly stratified reservoir regulated by floating intake. Exp. Therm Fluid Sci. 109, 109893. https://doi.org/10.1016/j.expthermflusci.2019.109893.
van Emmerik, T.H.M., Rimmer, A., Lechinsky, Y., Wenker, K.J.R., Nussboim, S., van de Giesen, N.C., 2013. Measuring heat balance residual at lake surface using Distributed Temperature Sensing. Limnol. Oceanog. Methods 11 (2), 79–90.
Vercauteren, N., Huwald, H., Bou-Zeid, E., Selker, J.S., Lemmin, U., Parlange, M.B., Lunati, I., 2011. Evolution of superficial lake water temperature profile under diurnal radiative forcing. Water Resour. Res. 47 (9) https://doi.org/10.1029/2011WR010529.
Walsh, J.R., Hansen, G.J.A., Read, J.S., Vander Zanden, M.J., 2020. Comparing models using air and water temperature to forecast an aquatic invasive species response to climate change. Ecosphere 11 (7). https://doi.org/10.1002/ecs2.v11.710.1002/ecs2.3137.
Wang, J., Huang, L., Ju, J., Daut, G., Wang, Y., Ma, Q., Zhu, L., Haberzettl, T., Baade, J., Mäusbacher, R., 2019. Spatial and temporal variations in water temperature in a high-altitude deep dimictic mountain lake (Nam Co), central Tibetan Plateau. J. Great Lakes Res. 45 (2), 212–223.
Wang, L.i., Shen, H., Wu, Z., Yu, Z., Li, Y., Su, H., Zheng, W., Chen, J., Xie, P., 2020. Warming affects crustacean grazing pressure on phytoplankton by altering the vertical distribution in a stratified lake. Sci. Total Environ. 734, 139195. https://doi.org/10.1016/j.scitotenv.2020.139195.
Weber, M., Rinke, K., Hipsey, M.R., Boehrer, B., 2017. Optimizing withdrawal from drinking water reservoirs to reduce downstream temperature pollution and reservoir hypoxia. J. Environ. Manage. 197, 96–105.
Woolway, R.I., Kraemer, B.M., Lenters, J.D., Merchant, C.J., O'Reilly, C.M., Sharma, S., 2020. Global lake responses to climate change. Nature Rev. Earth Environ. 1 (8), 388–403.
Woolway, R.I., Merchant, C.J., 2019. Worldwide alteration of lake mixing regimes in response to climate change. Nat. Geosci. 12 (4), 271–276.
Yang, Y., Deng, Y., Tuo, Y., Li, J., He, T., Chen, M., 2020. Study of the thermal regime of a reservoir on the Qinghai-Tibetan Plateau, China. PLoS One 15 (12), e0243198. https://doi.org/10.1371/journal.pone.0243198.
Yildirim, N., Kocabaş, F., 1998. Critical Submergence for Intakes in Still-Water Reservoir. J. Hydraul. Eng. 124 (1), 103–104.
Zarfl, C., Lumsdon, A.E., Berlekamp, J., Tydecks, L., Tockner, K., 2015. A global boom in hydropower dam construction. Aquat. Sci. 77 (1), 161–170.
Zhang, Y., Wu, Z., Liu, M., He, J., Shi, K., Wang, M., Yu, Z., 2014. Thermal structure and response to long-term climatic changes in Lake Qiandaohu, a deep subtropical reservoir in China. Limnol. Oceanog. 59 (4), 1193–1202.
Zhao, F., Frieler, K., Warszawski, L., Lange, S., Schewe, J., Reyer, C., Ostberg, S., Piontek, F., Betts, R.A., Burke, E., 2016. Assessing the impacts of 1.5°C of global warming - The Inter-Sectoral Impact Model Intercomparison Project (ISIMIP) approach.
Zhu, L., Wang, J., Ju, J., Ma, N., Zhang, Y., Liu, C., Han, B., Liu, L., Wang, M., Ma, Q., 2019. Climatic and lake environmental changes in the Serling Co region of Tibet over a variety of timescales. Sci. Bull. 64 (7), 422–424.
Zhu, S., Ptak, M., Choiński, A., Wu, S., 2020. Exploring and quantifying the impact of climate change on surface water temperature of a high mountain lake in Central Europe. Environ. Monit. Assess. 192 (1) https://doi.org/10.1007/s10661-019-7994-y.